

Research

Machine-learning algorithms for identifying climate-resilient corals in the Republic of Palau

Anderson B. Mayfield¹ · Alexandra C. Dempsey²

Received: 5 March 2025 / Accepted: 16 September 2025

Published online: 27 September 2025

© The Author(s) 2025 [OPEN](#)

Abstract

To restore degraded coral reef habitats, it is critical to ensure that the scleractinian broodstock utilized can withstand future heatwaves. However, reef coral resilience is normally assessed only after catastrophic stress events. By tapping into a rich, “molecules-to-satellites” dataset acquired during the Living Ocean Foundation’s research mission to the Republic of Palau, we trained an artificial intelligence to accurately predict pocilloporid coral thermotolerance from relatively cheap, easy-to-measure environmental and ecological survey parameters. Specifically, a neural network featuring 22 predictors, such as coral cover and colony size, could forecast the whereabouts and properties of climate-resilient colonies of *Pocillopora acuta* with ~90% accuracy. This machine-learning model enables practitioners to (1) estimate the climate resilience of local pocilloporid populations and (2) identify habitats characterized by high pocilloporid coral resilience.

Keywords Climate change · Corals · Ecological forecasting · Machine-learning · Resilience

Abbreviations

CHI	Coral health index
EF	Environmental factor (i.e., predictor)
FDR	False discovery rate
GCP	Genome copy proportion
GRE	<i>Global Reef Expedition</i>
GUI	Graphical user interface
HL	Hidden layer
HMS	Heat map score
mORF	Mitochondrial open reading frame
NN	Neural network
PAR	Photosynthetically active radiation
Sym	Symbiodiniaceae

Supplementary Information The online version contains supplementary material available at <https://doi.org/10.1007/s44289-025-00080-7>.

✉ Anderson B. Mayfield, anderson@coralreefdiagnostics.com; Alexandra C. Dempsey, dempsey@livingoceansfoundation.org | ¹Coral Reef Diagnostics, Miami, FL, USA. ²Khaled Bin Sultan Living Oceans Foundation, Annapolis, MD, USA.



1 Introduction

Although climate change threatens coral reefs across the globe [1], there are well established gradients in thermo-tolerance both across and within scleractinian species [2]. In some instances, extreme oceanographic conditions have led to coral stress-hardening; corals from (a) high-temperature pools in American Samoa [3] and (b) upwelling reefs of Southern Taiwan [4] have shown superior ability to acclimatize to both natural and experimentally induced temperature spikes. Unfortunately, many reefs historically thought to be relatively climate change-tolerant, such as those of the Red Sea, are now bleaching regularly [5], with normally more robust genera like *Porites* even amongst the thermo-sensitive reef-builders. There is nothing that can be observed in situ that signifies whether a particular colony is of high climate resilience prior to a marine heat wave. A practitioner probing a new region for the most thermotolerant colonies of a particular species needs to instead either conduct a laboratory-based thermal stress challenge requiring expensive equipment (e.g., CBASS [6]) or wait for a natural stress event to transpire to determine the biological material that may make the most sense to use as broodstock for selective breeding or coral reef restoration programs.

In remote regions where monitoring is not routinely undertaken, researchers may only have the chance to identify the most resilient corals by timing their expeditions to fall during hypothesized bleaching events (e.g., via consulting NOAA's [Coral Reef Watch](#) forecasts [7]) or instead attempting to identify habitats featuring oceanographic conditions known to stress-harden corals [8]. Since even uncovering whether such conditions exist in a given under-studied (or unstudied) area might be challenging, we attempted herein to “work backyards” from a holistic, “molecules-to-satellites” dataset acquired along the leeward (western) coast of the Republic of Palau during the Living Oceans Foundation's *Global Reef Expedition* (GRE [9]) to generate predictions of coral climate resilience from easier-to-measure parameters.

During this 2016 expedition, divers surveyed the coral reef benthos (0–35 m) using a standardized protocol [10], fish biomass and diversity assessments were conducted, reefs were mapped and integrated with satellite imagery [11], and colonies of the model coral *Pocillopora acuta* were sampled along the leeward reefscape. Their climate resilience was assessed via calculation of a “coral health index” (CHI) as described previously [12, 13], followed by fate-tracking a subset of colonies. CHI ranges from 0 (dead) to 5 (immortal) and scales positively and linearly with stress tolerance+longevity. However, it involves measuring many expensive (~\$500USD/sample) physiological and molecular response variables [14] that require highly trained personnel; it is neither a rapid nor a practical solution for those working in developing nations. We therefore sought to take a modeling approach to predict the CHI in unmeasured samples from cheaper environmental (e.g., habitat type, seawater quality), ecological (namely benthic composition), and “in situ physiological+morphological parameters” (i.e., those that can be measured underwater by divers). Our goal was to predict bleaching susceptibility without the need for laboratory analyses. If validated, the resulting models could aid restoration practitioners and others seeking knowledge on the whereabouts and properties of climate-tolerant corals in (1) expediting their search more strategically and (2) making superior projections about the future state of local reefs.

2 Materials and methods

2.1 Surveys and sample collection

Standardized protocols were used across all legs of the GRE, the largest coral reef survey to date, with key facets mentioned in Carlton et al. [10]. The benthic data can be found in a companion article [9], where we took a similar modeling approach to instead predict the whereabouts of unexplored reefs with high coral cover. The environmental and ecological parameters assessed are detailed in Table 1; readers interested in Palau's windward reefs, which were not visited due to high seas, should consult Colin [15]. Although 86 sites were surveyed (see Fig. 1 of Mayfield & Dempsey [9]), *P. acuta*-like corals were sampled from only 37. Because *Pocillopora damicornis* and *P. acuta* were still widely believed to be the same species at that time, colonies presenting either morphology (typically more corymbose & branching, respectively) were sampled, with a genetic test later used to confirm species. Briefly, ~50-mg branch tips (range = 40–150 mg) were removed by surgical bone-cutting pliers from each of 150 colonies spanning a number of

Table 1 Factors predicted to influence the coral health index (CHI) and coral lifespan.

Name	Abbreviation	Units	Options
MORPHOLOGICAL+PHYSIOLOGICAL FACTORS (PHYS)			
Maximum colony length	Max. length	cm	Continuous (range=4–41 cm)
Planar surface area ^a	Planar SA	cm ²	Continuous (range=9–508 cm ²)
Colony color	color	1–5; %	As either a mean score for the colony (1–5) or a percentage of the colony with anomalous pigmentation
Endosymbiont assemblage	Sym assemblage		<i>Durussidinium</i> , <i>Cladocopium</i> , <i>Symbiodinium</i> , or combinations thereof
Polyps extended?	–	NA	Yes or no
ENVIRONMENTAL FACTORS (ENV)			
Latitude	Lat	°N	Continuous (range=6.92–8.17°N)
Longitude	Lon	°E	Continuous (range=134–135°E)
Island ^a	–	NA	See Carlton et al. [10] (n = 10)
Survey site ^a	Site		See Fig. 1 of Mayfield & Dempsey [9]
Lagoon	–	NA	Inside or outside
Fore reef	–	NA	Is or is not
Reef emergence	Emergence	NA	Submerged or emergent
Reef exposure	Exposure	NA	Protected, intermediate, or exposed
Reef location	Location	NA	Lagoon, back reef, or fore reef
Reef type	Type	NA	Fringing reef, barrier reef, patch reef, back reef, or channel reef
Time (binned)	Time	NA	<10:00, 10:00–14:00, 14:00–18:30, or >18:30
Night?	–	NA	Yes or no
Temperature	Temp	°C	Continuous (range=26–29.4°C)
Salinity	–	None	Continuous (range=31–34.4)
Photosynthetically active radiation	PAR	μmol m ^{−2} s ^{−1}	Continuous (range=0–335 μmol m ^{−2} s ^{−1})
Colony depth	Depth	m	Continuous (range=5–31 m). As binned in 5-m increments in certain analyses (< 5 m, 5–10 m, etc.)
ECOLOGICAL (BENTHIC) FACTORS (ECO)			
% barren substrate	PB	%	Continuous (range=0.5–42%)
% non-coral invertebrates	PINVS	%	Continuous (range=1.2–20.6%)
% algal cover by taxon	6 taxa	%	See online supplemental data file (Appendix B)
% coral cover by genus	73 genera ^b	%	See online supplemental data file (Appendix B)
Total live coral cover	LCC	%	Continuous (range=13–70%). As binned in certain analyses: 10–20%, 20–30%, 30–40%, etc.
Total live algal cover	LAC	%	Continuous (range=12–71%)
Coral/algae ratio			Unitless (range=0.2–5.1)
#coral genera present	Sum (#genera)	n	Continuous (range=17–45 genera)
#coral genera present-binned	Sum (#genera)-binned	n	In 5-genera increments: < 5 genera, 5–10 genera, 10–15 genera, etc.

^aExcluded from most analyses.

^bOnly 63 were observed in the vicinity of the sampled coral colonies.

habitat characteristics (Table 1). Care was taken to ensure at least 10-m separation between colonies to reduce risk of sampling clonemates [16]. Each biopsy was broken in two: one was placed in a cryo-tube and rapidly frozen in a liquid nitrogen (-150°C) dry-shipper (Chart MVE, USA), and the second was coated with 1.5-ml of RNALater™ (Life Technologies, USA) and frozen at -80°C for 1–2 weeks before later transferring to the dry-shipper. The samples were exported under a CITES permit issued by Palau's Bureau of Marine Resources and then imported to Taiwan several days later, where they were stored in 1 ml of TRIzol™ (Thermo-Fisher Scientific, USA) at -80°C until the time of extraction.

With the exception of the Symbiodiniaceae (Sym) assemblage, all other parameters can be determined by eye, via cheap ($< \$100\text{USD}$) meters deployed in situ (e.g., temperature & photosynthetically active radiation), or in silico (e.g., ImageJ [NIH, USA] for determining colony size). Note that certain seawater quality parameters that have large implications for coral health, namely temperature and salinity, were included as predictors, though variation was low for both given the short-term nature of the field trip. NA: not applicable.

2.2 Coral biopsy extractions and molecular response variables

In addition to two morphological and two physiological response variables that were documented in situ (or via assessment of images on a computer)-maximum (max.) colony length, planar surface area, color [17], and polyp extension (expanded or retracted)-several biomarkers were measured to calculate the CHI after extracting RNA, DNA, and protein from a subset of 118 of the 150 biopsies as described previously [18]. Briefly, a modified TRIzol method was used which first involved complete pulverization of the coral tissue+skeleton biopsies directly in $\sim 1\text{--}2$ ml of TRIzol in a pre-sterilized mortar in a fume hood. After several minutes of room temperature incubation, 0.2 ml of chloroform were added, and samples were vortexed and spun at $12,000 \times g$ for 10 min at 4°C (hereafter simply referred to as “spun”). Next, RNAs (~ 0.5 ml) within the upper aqueous layer were isolated via careful pipetting, precipitated with a high-salt solution (0.25 ml of 0.8 M Na citrate+1.2 M NaCl) and isopropanol (0.25 ml) at -20°C for several hours (or sometimes overnight), and then either (a) washed with 75% ethanol, spun, dried on the benchtop, and resuspended in 30 μl of DEPC-treated water or (b) purified with the GeneMark Plant Total RNA minikit (Taiwan) and eluted in 30 μl of DEPC-treated water.

DNAs were co-extracted from the same TRIzol+coral biopsy homogenized tissue. After removing the RNA aqueous layer, 0.5 ml of a “back extraction buffer” [18] were added, and samples were vortexed, incubated on a shaker table for 20–30 min, and spun. Then, the aqueous layer containing the DNA was removed as above, precipitated in isopropanol at -20°C for several hours (or overnight), spun, dried, resuspended in 100 μl of Buffer A from the Axygen (USA) PCR clean-up kit, and then purified through a spin column per the manufacturer's recommendations. The co-extracted DNAs (eluted into 50 μl of manufacturer's elution buffer, likely to be Tris-HCl [pH 8] or Tris-EDTA buffer) were used for four purposes. First, a multiplex Taqman® assay from Thomas et al. [19] was employed to species-type the coral hosts. From this same DNA aliquot, the Symbiodiniaceae assemblage (to genus-level) was elucidated as in Correa et al. [20]. Next, the Symbiodiniaceae genome copy proportion (GCP), a molecular proxy for endosymbiont density, was calculated via real-time PCR as in a prior work [21]. Briefly, this assay features measuring the genomic copy numbers of the same gene ortholog, heat shock protein 70 (*hsp70*), in both the coral host and the dinoflagellate endosymbionts, with the latter divided by the sum of both. Upon multiplying by 100 (to generate a percentage), the resulting value reflects the relative proportion of nucleic acids and other macromolecules in the extract pool that were of endosymbiont origin. This is important because Symbiodiniaceae cells are difficult to lyse, and variable quantities of endosymbiont macromolecules amongst samples can bias gene expression and other molecular analyses.

The co-isolated proteins were precipitated overnight at -20°C in 2 ml of acetone, spun, and the acetone was decanted. Then, 1 ml of 0.3 M guanidine HCl in 95% ethanol with 2.5% glycerol were added to the pellets, which were sonicated on ice for several minutes or until the pellets had completely dissociated into a uniform, milky consistency. These precipitated and incompletely washed proteins were stored at -80°C for a future comparison of light versus dark proteomes (a subset of colonies was sampled both during the day & again at night.).

Coral host and dinoflagellate endosymbiont biomarkers determined to be stress-responsive from prior transcriptomic analyses [22] are discussed in detail with respect to their use in calculation of the CHI in prior works [12, 13] and are shown in Table 2. They included four stress-responsive coral host genes—copper-zinc superoxide dismutase (*cu-zn-sod*; involved in oxidative stress), catalase (also involved in the oxidative stress response), cytochrome P450 (involved in detoxification), and green fluorescent protein-like chromoprotein (*gfp-cp*; hypothesized to play a role in host coral self-shading), and four Symbiodiniaceae genes: ubiquitin ligase (*ubig-liq*; cellular stress response [CSR]), heat shock protein 90 (*hsp90*; CSR), catalase-g (*katG*; CSR & oxidative stress), and zinc-induced facilitator-like 1-like (*zifl1*; unknown function but documented at high levels in multiple studies of environmentally stressed coral-dinoflagellate holobionts [23]).

2.3 Coral health index (CHI)-details

The CHI involves averaging four metrics of coral performance as follows. A “heat map score” (HMS) is first calculated across the 10 univariate response variables (RNA/DNA ratio, Symbiodiniaceae GCP, four host coral gene mRNAs, & four endosymbiont RNAs [Table 2]); this is akin to summing all response variables that fell outside the normal range for a healthy coral. For instance, if two thermal stress biomarkers fell outside the normal reference range (Table 2), the biopsy would receive an HMS of 2. The second parameter used in the calculation of the CHI is the “color metric,” which is the average of the inverse-standardized color score (since high color scores are indicative of healthy corals, & we aimed for the color metric to scale to where high values are reflective of stressed corals), the inverse-standardized Symbiodiniaceae GCP, and the standardized tissue necrosis score (the percentage of the colony with either completely bleached or necrotic tissue). The variability index is the third parameter used in the calculation of the CHI; this is simply the standard deviation across the standardized means of all continuous response variables used in calculation of the HMS. As higher variation is indicative of loss of control of homeostasis, higher variability index values reflect corals of compromised health. Finally, the Mahalanobis distance is calculated to serve as the multivariate counterpart to the variability index, indicating the degree of multivariate deviation from normal behavior; high Mahalanobis distances are strong evidence for physiological stress.

The HMS, color metric, variability index, and Mahalanobis distance were each standardized across all samples individually, averaged for each individual, and then standardized again across all pocilloporid coral samples. The resulting values were then multiplied by -1 since the CHI scales to where low values are for stressed corals and high values are for resilient ones. These values were next converted to normal quantile scores, then range-scale-adjusted to where they spanned 0–1. Finally, these values were multiplied by 5 to yield the final CHI scores. In the example shown in Table 2, the respective z-scores of the HMS, color metric, variability index, and Mahalanobis distance are 1.2, 0.2, 3.5, and not estimable (the Mahalanobis distance cannot be calculated with missing data, & not all response variables were measured for this sample.), respectively. The three values would be averaged (1.6), assessed against the respective means of all other samples, and once again standardized: -2.5 . This value would then be converted to a normal quantile score (-1.7), range-scaled from 0 to 1 (0.16), and then multiplied by 5 to yield a CHI of 0.8, which is evidence for extreme physiological stress.

2.4 Predictive modeling

An approach analogous to that of Mayfield et al. [14] was taken to attempt to predict the CHI from combinations of cheaper and easier-to-measure environmental and ecological parameters (i.e., “predictors”). These include those of Table 1 and subsets thereof (discussed in Appendix B-sheet “model terms”). A two-step approach was taken in JMP® Pro (USA), which was used for all statistical and modeling analyses. First, JMP Pro’s “model screening” platform was used to simultaneously generate and compare a large number of models—decision tree, stepwise regression, generalized regression, bootstrap forest, boosted tree, Naïve Bayes, discriminant, XGBoost, support vector machines, partial least squares, k-nearest neighbors, neural network, and others—with CHI as the Y and second-order factorial combinations of subsets of predictors as the X’s (Tables A1–A2 in Appendix A). CHI was modeled three different ways: as a continuous value spanning 0–5, as binned into categorical scores of 0, 1, 2, 3, or 4–5 (values rounded to the nearest integer), or as a colony being either weak ($\text{CHI} \leq 1$) or resilient (> 1). The data table was randomly partitioned into 89 (75%) and 29 (25%) training and validation samples, respectively, and all error terms below represent std. dev. Of the latter 29 colonies, a random subset of 22 (those accessible by small-craft diving vessels) were tagged and fate-tracked for one year (2016–2017) to field-test the models; this is critical given that neural networks are prone to over-fitting data even when holdback validation is performed, especially considering that there were nearly as many predictors as samples in the case of the PHYS+ENV+ECO models (Appendix A).

When the superior modeling type identified—defined as the one with the highest validation data R^2 for the continuous CHI analyses (acceptance threshold > 0.8) and the highest accuracy for the categorically binned health values (acceptance threshold $> 90\%$)—was a neural network, a tuning GUI developed by Diedrich Schmidt was used to test hundreds to thousands of combinations of the core neural network hyperparameters (e.g., number of hidden layers, learning rate) as described previously [24]. Specifically, the following hyperparameters were tuned using a classic design-of-experiments approach: number of hidden layers (1 or 2), types of activation (tanH, linear, or Gaussian), number of nodes of each activation type within a layer (0, 1, 2, or 3), boosting (0 [none] to 30, but only > 0 for single hidden-layer models), learning rate (0.05–0.3), transformed covariates (yes or no), robust fit (yes or no), penalty method (weight decay, squared, absolute, or none), and number of tours (1–200). Of these, the degree of boosting and the number of tours have had the greatest

impact on the performance of neural networks seeking to predict changes in coral health [9, 14, 24]. In addition to creating a validation column stratified by coral health status or CHI as described above, kfold (5) validation was sometimes used to ensure that random partitioning of the dataset (training vs. validation) in multiple iterations consistently yielded models with satisfactory validation R^2 (or misclassification rates for categorical Y's) while simultaneously minimizing the chance of over-fitting (a significant concern for neural networks [24]). In these cases, the model performance parameters were averaged across the five folds (as opposed to taking the results from the fold that yielded the superior predictive performance).

Another analysis was undertaken in which images of the sampled corals at both mm- and cm-scales were analyzed alongside the other predictors to determine whether the powerful Torch AI could uncover image features that are diagnostic of particular health states. In general, Torch did not outperform neural networks (Table A3), though it is important to note that, for image analysis AIs to be properly leveraged, care must be taken to standardize image parameters *in situ*, such as distance from the colony, light level, etc. Many of these conditions might only lend themselves to laboratory analyses at present.

2.5 Code and data availability

In addition to including all data analyzed in the manuscript, the Python scripts needed to run the two superior neural network models discussed below have been included in the online supplemental data file (Appendix B). Images of all sampled coral colonies, as well as habitat photos of the surrounding reefs, can be found on coralreefdiagnostics.com under the "Palau" menu. Physiological data have been overlaid on images of each colony (including those excluded from analysis herein due to missing data). For those unfamiliar with running Python scripts, a GUI featuring the most parsimonious model discussed has been embedded as an iframe on <https://coralreefdiagnostics.com/palau-bioprospecting>.

3 Results

3.1 Coral species-typing

All sampled colonies were typed as *P. acuta*, and not *P. damicornis*; based on our benthic survey data, it is doubtful that *P. damicornis* is present in the west of Palau. To verify whether the probe-based assay of Thomas et al. [17] was accurate, the mitochondrial open reading frames (mORF) of three random DNA samples were PCR-amplified and sequenced in both directions, and all were 100% matches to published *P. acuta* mORF sequences on the NCBI database.

3.2 Predictor screening

Reef site was found in > 2 of the 100 random bootstrap forest models generated during the predictor screen and was the most influential predictor of CHI (Fig. 1a); however, because our goal was to produce a generalizable model that could be used to find resilient corals in sites *not-yet-surveyed*, we removed this term from subsequent analyses. Of the remainders, Symbiodiniaceae assemblage requires molecular benchwork and is discussed in more detail below. Max. colony length and surface area co-vary (quadratic relationship; $R^2 = 0.90$, $p < 0.0001$) since both are proxies of colony size; as such, their relative influences on the CHI are similar.

3.3 Response screening

A response screen is a false discovery rate (FDR)-controlled means of looking at each individual predictor's influence on a Y, and only a single predictor, *Pachyseris* spp. cover (Fig. 1b), was associated with a p -value < 0.01. However, this correlation was not statistically at the FDR-adjusted p -value of 0.1, and cover of this genus explained only ~8–9% of the variation in the CHI. Although it may be tempting to interpret this inverse relationship as evidence for competition, confounding factors are likely responsible; *Pachyseris* is a low-light coral found at depths > 20 m, whereas *P. acuta* is more common in the shallows. Those areas where the former is relatively more abundant are likely to be associated with lower CHI scores for *P. acuta*.

3.4 Variation in CHI

Because reef site was the top predictor in the predictor screen, we plotted CHI across an $0.1 \times 0.1^\circ$ grid (Fig. 2a). Although variability can be observed, there were no clear trends with respect to latitude, longitude, proximity to land, or other geographic variables that would be useful to managers. There was also no correlation between CHI and either total live coral (Fig. 2b) or pocilloporid cover (Fig. 2c); simply documenting the abundance of these corals, as is the extent of most surveys [25], is insufficient for making predictions of climate resilience. In fact, the few remaining corals in a highly marginalized habitat could be expected to *outperform* conspecifics from relatively less impacted areas [26].

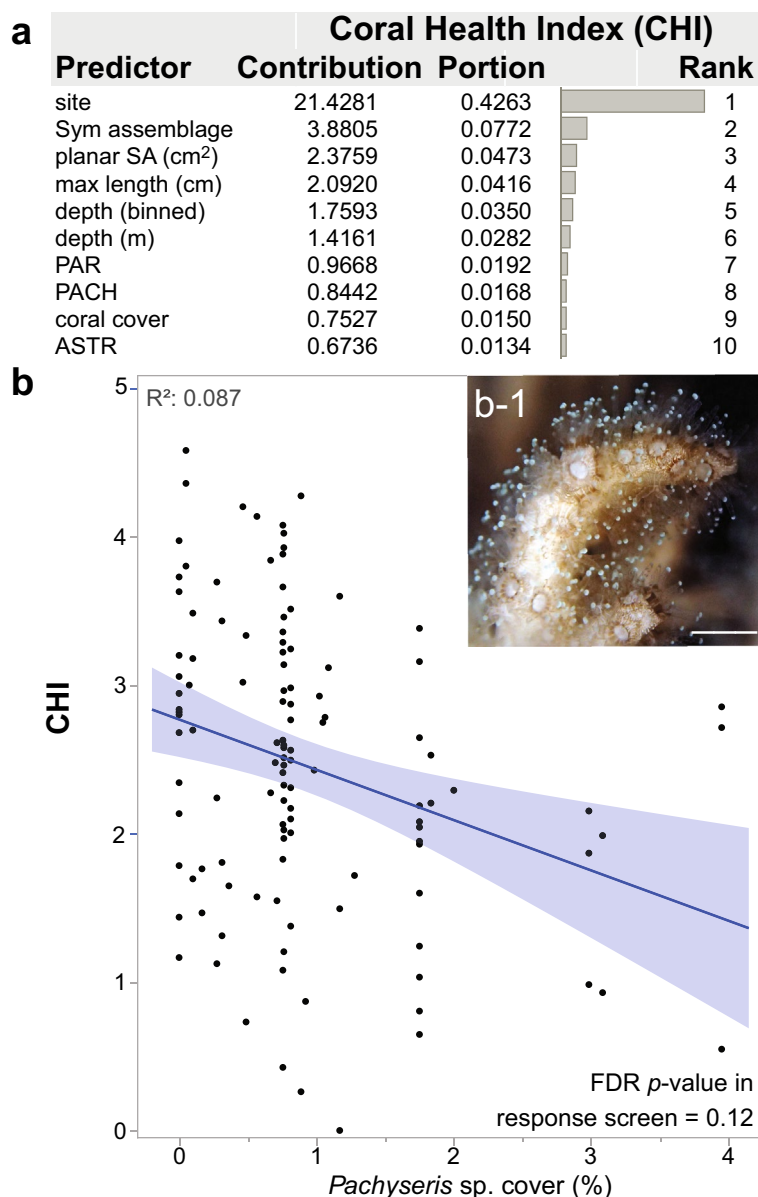


Fig. 1 Predicting the coral health index (CHI) from common physiological/morphological+environmental ($n=22$) and ecological ($n=77$) parameters (all of which being relatively easier & cheaper-to-measure than the CHI itself). The physiological/morphological and environmental predictors included those 4 and 16 in Table 1 ($n=20$), respectively, as well as #21) depth binned into pre-defined categories and #22) site. The ecological parameters included those 76 of Table 1 plus #77) coral cover binned into 10-% increments (10–20%, 20–30%, etc.). Only the top 10 predictors have been shown (a). CHI was plotted against the top predictor identified in the response screen: *Pachyseris* spp. (“PACH” in [a]) abundance (b). The shading about the line-of-best fit represents 95% confidence. A thinly branched *Pocillopora acuta* sample with a relatively high CHI score (> 3.5) has been shown in b-1. Scale bar=3 mm.

Table 2 Diagnostic results for a representative sick coral: PaPd21.1–2. Although the same data were collected from pocilloporids of other *Global Reef Expedition* missions, the reference (Ref) range is local to Palau. The color score, % of colony bleached/necrotic, and Symbiodiniaceae (Sym) genome copy proportion (GCP) were used to calculate the "color metric." Full gene names are as follows: copper-zinc superoxide dismutase (*cu-zn-sod*), green fluorescent protein-like chromoprotein (*gfp-cp*), ubiquitin ligase (*ubiq-ligase*), heat shock protein 90 (*hsp90*), catalase-peroxidase (*katG*), & zinc-induced facilitator-like 1-like (*zifl1*). NA: not applicable. NM: not measured

Response variable	Value	Ref range	In spec?	Diagnosis/notes
Colony color score	5	> 4	Yes	Normal appearance
% of colony bleached/necrotic	0	< 10	Yes	No evidence of bleaching or disease
Max. colony length	27	(4, 41)	Yes	
Planar surface area	220	(9, 508)	Yes	
Polyps extended?	Yes	Yes	Yes	
The following 10 response variables were used to calculate the heat map score:				
RNA/DNA ratio	1.93	> 0.5	Yes	
Sym GCP	0.05	(0.05, 5)	Borderline	Low endosymbiont densities despite normal appearance; evidence of non-dinoflagellate algae?
Host coral <i>cu-zn-sod</i>	0.91	(0.5, 1.5)	Yes	
Host coral <i>gfp-cp</i>	0.05	(1, 6)	Too low	Could point to compromised ability to self-shade
Host coral cytochrome P450	0.01	(0.02, 0.4)	Too low	Could point to problems with host metabolism
Host coral catalase	1.5	(0.5, 5)	Yes	
Sym <i>ubiq-lig</i>	10.2	(0.01, 0.3)	Too high	Strong evidence for endosymbiont stress response
Sym <i>hsp90</i>	15.9	(0.1, 10)	Too high	Strong evidence for endosymbiont stress response
Sym <i>katG</i>	1.1	(0.01, 5)	Yes	
Sym <i>zifl1</i>	NM	(1, 100)	NA	Extracted insufficient RNA to measure this mRNA
The following four metrics were used to calculate the CHI:				
Heat map score	3	(0, 2)	Too high	
Color metric	0.17	> -0.7	Yes	
Variability index	2.8	< 1	Too high	Evidence for loss of control of homeostasis
Mahalanobis distance	NM	(1, 4)	NA	Could not calculate due to missing data
CHI	0.8	> 1	Too low	Diagnosis: colony is abnormally stressed Prognosis: colony will not survive future heat wave Outcome: colony perished after subsequent heat wave

NA: . NM t measured

3.5 A neural network for predicting CHI-a: 23-predictor model (Fig. 3)

Because the CHI (as continuous & binned as five integers) could not be confidently predicted ($R^2 < 0.8$ & misclassification rate $> 10\%$, respectively; Table A1), corals were scored as either resilient ($\text{CHI} > 1$) or weak ($\text{CHI} \leq 1$; "sick" in some tables & figures), and models approached 97% accuracy when including virtually all environmental and ecological predictors (Table A2); 100% of the models surpassing the 90% accuracy cutoff were neural networks. A more parsimonious model is shown in Fig. 3. In this single-hidden layer, boosted neural network featuring Gaussian activation (Fig. a), 91% accuracy was achieved in predicting whether a coral would perish from or resist bleaching, and only 23 environmental factors were incorporated as X's; this represents only a ~6% drop in accuracy whilst needing ~four-fold less data than for the 97%-accuracy model. In the subset of field test samples ($n=22$ colonies), 5 (25%) were predicted to perish by summer of 2017, and all did (100% accuracy); 1 of the remaining 17 was a "false-positive:" predicted to be climate-resilient but actually died (95% accuracy across the 22 colonies).

The 23 environmental factors featured in this model have been listed with respect to their total effect in the independent uniform inputs variable importance analysis in Fig. 3b. A desirability analysis was conducted in which the AI was prompted to generate the conditions resulting in the highest probability of a coral being climate-resilient (" $p(\text{resilient}) = \text{maximized}$ "); T^2 extrapolation control was implemented to ensure that environmentally unrealistic conditions were not generated (e.g., an exposed lagoonal patch reef). By modifying the 23 predictors, a scenario was forecasted in which there is near-100% certainty that a coral would be climate-resilient; the results of the top-five predictors and

Fig. 2 Large-scale spatial variation in the *Pocillopora acuta* coral health index (CHI) in Palau. In panel **a**, means were calculated within $0.1 \times 0.1^\circ$ squares. Panels **b** and **c** show the correlation between CHI and total live cover of (1) all observed hard coral genera and (2) pocilloporid corals only, respectively. Bands about the regression lines represent 95% confidence, and neither correlation was statistically significant ($p > 0.01$).

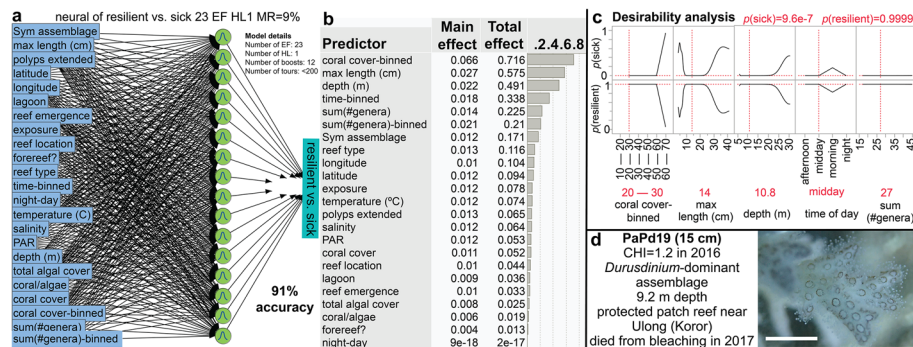
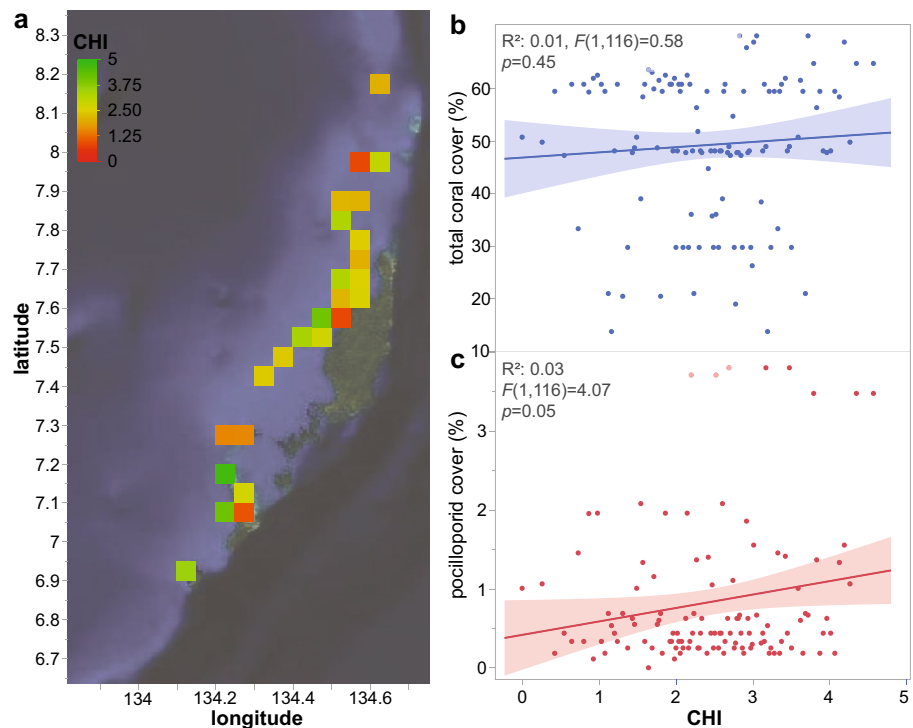
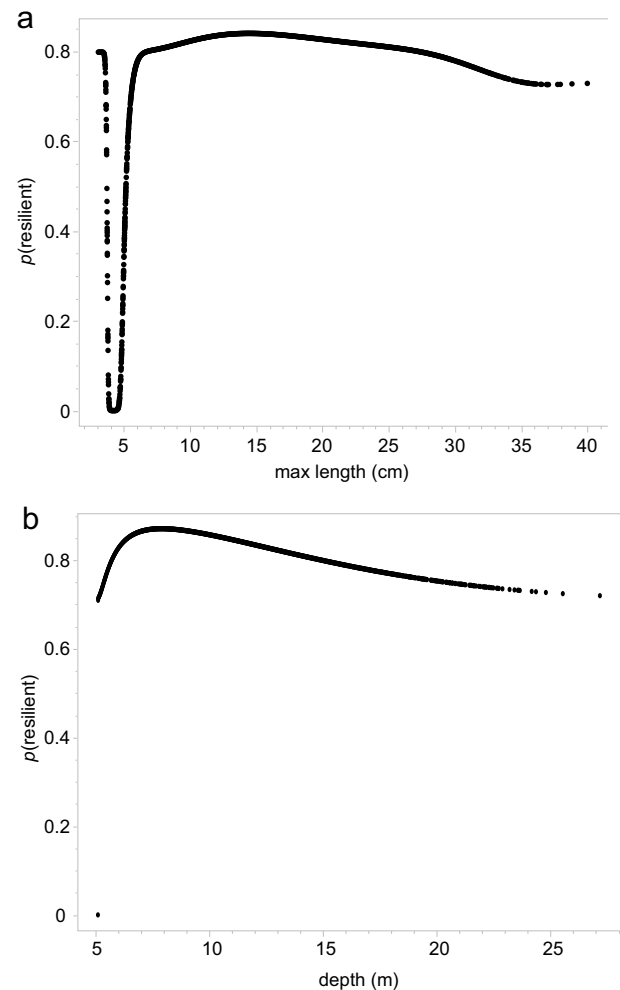


Fig. 3 A neural network for predicting coral resilience from 23 environmental factors (EF). The structure of the single-hidden layer (HL), Gaussian activation, boosted neural network is shown (**a**), with other hyperparameters presented in an inset; see Table A2 for additional model details. Results from a variable importance analysis (independent uniform inputs) are shown in (**b**) and reflect relative model weights of the various EF. A desirability analysis was performed with all 23 EF (**c**) to maximize the probability of a coral being climate-resilient ($p(\text{resilient})$). The optimal values for the top-five EF are written in red below the plots and shown in the plots themselves as hatched, vertical red lines. A colony with a markedly low coral health index (CHI) of only 1.2 (**d**), which perished on account of anomalously high temperatures in the year following its sampling (2017), has been shown (scale bar = 5 mm).

their optimal levels are shown in Fig. 3c. Coral cover had the greatest weight in the model, despite the fact that there was no clear relationship between CHI and coral cover in the simple, univariate approaches (Fig. 2b, c). However, the CHI did not vary across coral cover bins less than 60%; in other words, *P. acuta* resilience only plummets on reefs whose total live coral cover is > 60% (15 out of the 86 surveyed reefs). As reefs with coral cover over 60% would be very space-limited environments, competition with other corals could account for this decline in CHI.

Of the remaining four predictors in Fig. 3c, the horizontal line for summed coral genera is deceiving because the variable importance analysis clearly points to an influence of this diversity metric. This discrepancy is in part due to the fact that generic diversity covaries with several other environmental factors, such as coral cover ($R^2 = 0.05$); changes in other parameters confound that of generic diversity to where, under the projected conditions of the desirability analysis, $p(\text{resilient})$ does not vary. When performing a simulation (10,000 rows) and allowing generic diversity to fluctuate randomly across the entire range documented in Palau, there is a ~6% decrease in $p(\text{resilient})$ upon increasing the generic

Fig. 4 Simulated data ($n=10,000$) in which the optimal levels of the environmental factors (i.e., predictors) of the neural network in Fig. 3 were fixed with the exception of maximum (max.) colony length (a), which was allowed to vary randomly across a distribution with mean= 17 ± 8 cm, or colony depth (b), which was allowed to vary randomly across a distribution with mean= 15 ± 7 m.

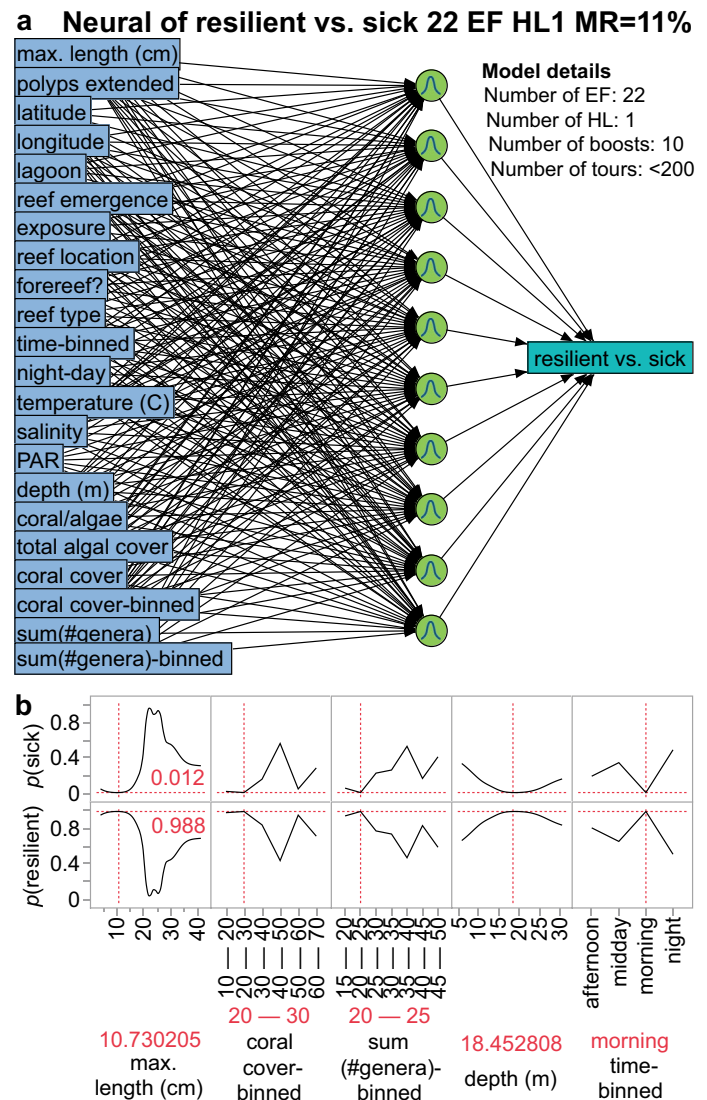


diversity from the optimal level of 27 genera to 41 genera (1.5-fold increase); in other words, generic diversity is a relatively weak predictor of *P. acuta* climate resilience when assessed by itself.

The optimal colony diameter of 14 cm (Fig. 3c) is significantly different from the mean colony size in Palau of 17 cm (± 8 cm; $p < 0.0001$). Since a typical colony can extend its diameter by ~ 2 cm per year [27], this 3-cm difference between the optimal and mean coral diameter represents a ~ 1.5 -year age difference. Why a slightly younger and smaller colony would have higher climate resilience is currently unclear, and upon looking at the various physiological response variables assessed (e.g., gene expression, Symbiodiniaceae density, etc.), few showed variation across size. Therefore, a simulation was run in which the other optimized parameters from the desirability analysis were fixed at their optimal levels while max. colony length was allowed to vary randomly across its Palauan distribution. The results (Fig. 4a) reveal that $p(\text{resilient})$ actually does not vary much once a colony reaches ~ 10 cm. There is a “danger zone” of 2–5 cm, possibly due to corallivory or lack of ability to effectively compete whilst at such a small size. Note that while Fig. 4a corroborates the findings of Fig. 3c at the lower end of the size range, the latter analysis shows another increase in the probability of colony being sick beyond about 30 cm that is only partly reflected in Fig. 4a. This discrepancy is likely due to the low number of large colonies sampled (only one was > 30 cm in diameter.).

Colony depth was also weighted highly in the superior predictive model of coral resilience (Fig. 3b), and the optimal depth was 10.8 m ($\text{PAR} = 91 \mu\text{mol m}^{-2} \text{s}^{-1}$), significantly shallower than the mean sampling depth of 15 m (± 7 ; $\text{PAR} = 77 \mu\text{mol m}^{-2} \text{s}^{-1}$). However, this is close to the median depth of 10.9 m (due to the highly skewed nature of the dataset, in which most corals were collected in the 8–12-m window). PAR alone did not have a strong impact on CHI or $p(\text{resilient})$ (Fig. 3b). Wave energy (as “exposure” in the tables & figures), which would also vary by depth, was also a relatively weak predictor. From the desirability analysis (Fig. 3c), there is not a large decrease in $p(\text{resilient})$ until the depth increases to about 25 m. To attempt to corroborate this, another simulation was performed (10,000 samples) in which the

Fig. 5 Neural network (single-hidden layer [HL]) for predicting coral resilience (resilient vs. weak/sick) from 22 environmental factors (EF). The structure of the neural network has been shown (a) followed by a desirability analysis (b) in which the AI was programmed to maximize the probability of a coral being climate-resilient: $p(\text{resilient})$. Only the top-five EF from a variable important analysis (independent uniform inputs) have been shown, and the values in red below the plots, as well as the hatched, red, vertical lines in the plots themselves, represent the optimal values (at which $p(\text{resilient}) = \sim 99\%$). MR=misclassification rate.



optimal values were locked for all parameters except depth, which was allowed to fluctuate randomly across its Palauan dataset range. The results (Fig. 4b) are similar to those of Fig. 3c, albeit with a more gradual tapering at greater depths in the simulation. Another key difference is that the optimal depth in the simulation is notably lower, with $p(\text{resilient})$ maxing out at around 8 m instead of 11 m.

3.6 A neural network for predicting CHI-b: 22-predictor model (Fig. 5)

Were one interested in maximizing the chance of selecting a climate-resilient *P. acuta* colony in Palau, they would look for colonies around 14 cm in diameter at around 10–11 m depth in an area of relatively low (for Palau) (1) coral cover (20–30%) and (2) generic diversity (25–30 genera). All of these predictors can be assessed by diving equipment (depth gauge), simple scientific instruments like rulers (colony size), or trained surveyors (coral cover & generic diversity). However, there is a drawback to the model of Fig. 3; despite the fact that Symbiodiniaceae assemblage has a relatively low total effect size (~four-fold lower than coral cover, for instance), if removed from the model, the accuracy could decrease. Because Symbiodiniaceae assemblage requires laboratory benchwork that normally occurs days to weeks after a field trip is completed, it is not a desirable predictor for one looking for a fast, cheap means of identifying resilient corals. For this reason, the term was removed, and a similarly structured neural network was rebuilt (Fig. 5a); upon removing this expensive, difficult-to-measure response variable, the accuracy decreased to 89%, just lower than the *a priori* accuracy cutoff of 90%. This 2% decrease in accuracy may be worth sacrificing given that the resulting model features only metrics

that can either be assessed *in situ* or shortly after the dive upon analysis of image and benthic survey data. In fact, the top-five predictors are the same as in the model of Fig. 3, albeit with a different relative ordering. As with the 23-predictor model (Fig. 3c), the desirability analysis (Fig. 5b) recommends a relatively small colony (11 vs. 14 cm in Fig. 3) on a low coral cover reef (20–30% coral cover in both models) with relatively low coral diversity (20–25 genera vs. 27 genera in Fig. 3). The main difference between the two models is the recommended depth: 18.5 versus < 11 m in the models of Figs. 3 and 5, respectively; in other words, small resilient colonies (11 cm) prefer deeper habitats (18.5 m) than larger (14 cm) resilient colonies (10–11 m).

4 Discussion

4.1 Bioprospecting for resilient *P. acuta* colonies

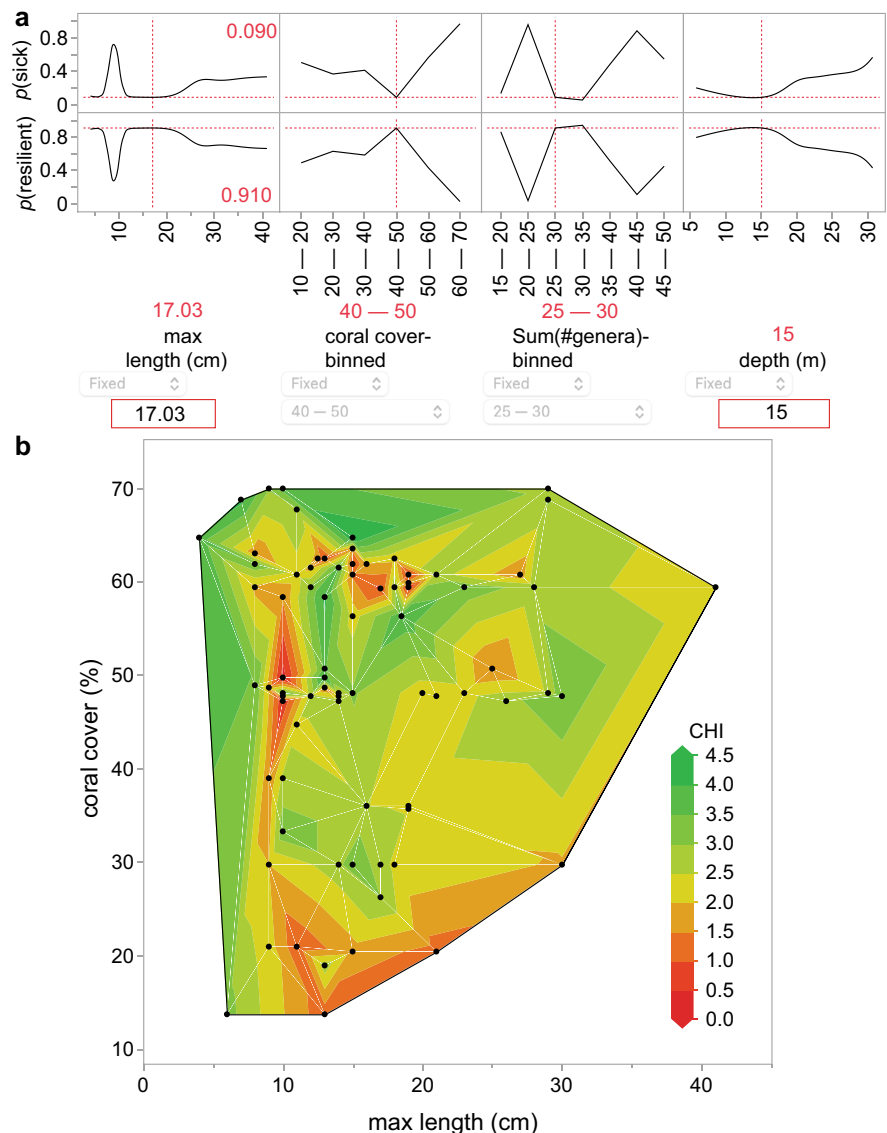
Machine-learning models are notoriously complex and difficult-to-interpret. That being the case, where should a practitioner interested in identifying resilient *P. acuta* colonies in Palau search? When relying upon the model in Fig. 3, a good start would actually be a reef with relatively low (for Palau) coral cover. This may seem counter-intuitive because historically we have equated high-cover reefs with being “healthier” [28]. However, a monoculture of *Acropora* sp., for instance, will likely have a very low tolerance to rapidly rising temperatures. In contrast, stress-hardened survivors at a reef with 5–10% live coral cover could very well be those that stand the best chance to withstand future heatwaves [26]. Furthermore, lower cover of other corals also means less competition and so the fact that the two superior models recommended 20–30% is unsurprising. From Fig. 3, it is evident that on the highest-coral cover reefs, the probability of identifying a physiologically compromised *P. acuta* colonies increases dramatically. Similarly, the optimal generic diversity for a site comprised of resilient *P. acuta* colonies is on the low end of the distribution in the desirability analyses of Figs. 3 and 4; this may also stem from the fact that higher coral diversity would equate to more potential competitors of *P. acuta*, in which case colonies might become weakened by, for instance, having to exert energy to defend themselves. Because *P. damicornis* and *P. acuta* were long synonymized, habitat preferences from prior studies, assessable on Coraltraits.org, are currently suspect, though the common nature of *P. acuta* on reefs and as a model coral for research [29] means that we can soon compare these results to simpler, habitat suitability models [30] from other regions to see if there are common environmental preferences linked to the most climate-resilient *P. acuta* colonies.

4.2 Predictive model evaluation and prospective utility

In even the top two neural networks, post-survey analyses must be performed to calculate coral cover and coral generic diversity; whether or not a particular reef habitat is colonized by resilient *P. acuta* specimens would, in other words, not be known until after the dive, and a repeat visit would be necessary to collect samples (were the conditions indeed even suggestive of resilient corals). What is more likely to be the case is that a scientist or manager will have some pre-existing data on certain reefs, such as a long-term monitoring site. In this case, the relevant values can be put into the model of Fig. 5 (as a GUI) to calculate the probability that a particular habitat might be characterized by resilient pocilloporids. As a hypothetical example, say that a surveyor determined that a particular reef area is characterized by a coral cover of 40–50% with 25–30 coral genera present and pocilloporid corals found around 15 m. By inputting these values into the model of Fig. 5 and setting them as “fixed,” we can then re-calculate $p(\text{resilient})$ across differing colony sizes. Under these conditions, a colony of 17-cm diameter would have a 91% chance of being climate-resilient (Fig. 6a); were coral cover and colony size instead allowed to vary, while the other 20 environmental parameters are fixed at their optimal levels, a contour plot (Fig. 6b) instead provides a means of searching for resilient corals.

However, the model of Fig. 5 is contingent upon measuring all 22 environmental factors; what if there is insufficient time to do so? Some can be known from consulting maps (e.g., reef type, reef exposure), yet others require divers or at least drone or satellite imagery. If one knew all mapping-related parameters—latitude, longitude, lagoon (inside vs. outside), reef type, reef emergence, reef exposure, forereef (is or is not a forereef)—in addition to coral cover and pocilloporid colony depth, but did *not* know the abundance of any other organism or anything about the seawater quality, the probability of correctly finding a climate-resilient pocilloporid would be ~71%. If temperature and coral polyp extension were also known, the probability increases to 75%. If one did not know the sizes of the pocilloporid colonies, the probability decreases only slightly to 72%. Whether or not a proper survey of the benthos is worth the effort of increasing the probability of correctly sourcing resilient corals from 75 to ~90% will ultimately be up to the practitioner.

Fig. 6 A hypothetical analysis in which a practitioner can enter specific values for maximum (max.) colony diameter and/or depth into the model of Fig. 5 (a), while coral cover, coral generic diversity, and the remaining 18 environmental factors are fixed at the optimum levels from the desirability analysis. In this example, pocilloporids were common at 15 m. Upon entering “15” into the red box below “depth (m)”, the probabilities then update accordingly, and it was found by manually dragging the vertical, hatched red line in the max. colony length panel that, under these conditions, the colony size with the highest probability of being climate-resilient ($p(\text{resilient})=0.910$) under the conditions shown in **a** is 17 cm. Assuming all 20 EF except max. colony length and coral cover are fixed at their optimal levels, a contour plot (**b**) can be used to visualize scenarios associated with pocilloporids of high climate resilience (as the continuous coral health index [CHI]).



The value of an AI trained with data from 2016 may be suspect, especially considering that coral reefs have become increasingly marginalized since then; are predictions that were accurate in 2016–2017 of any use to us nearly 10 years later? Under the most pessimistic view, this dataset might only have value in highlighting what these reefs looked like when they were still dominated by stony corals; coral cover averaged ~45% on Palau's leeward reefs at that time, which is relatively high by global standards. Of the 118 pocilloporids analyzed in detail, 36 (31%) were predicted to perish from climate change-related temperature increases and/or local stressors; this includes 5 fate-tracked colonies, all of which died (100% accuracy). Of these 22 fate-tracked colonies, 17 were predicted to be climate-resilient, though 1 (PaPd92) was found dead in follow-up surveys in 2017 (“false-positive”). Although the site itself, a protected, lagoonal patch reef, was not exceptional, this relatively deep (28 m) colony was pale but characterized by a 1.5-fold higher Symbiodiniaceae density than an average coral in the region (despite an overall CHI of 2.9); this could be evidence for lack of host control of dinoflagellate growth, which would then compromise resilience. Interestingly, this colony was misclassified by both the simpler model (Fig. 3) and the more holistic one (Fig. 5).

The resulting overall field accuracy of 21/22 (95%) is similar to the validation sample accuracy (i.e., samples simply held back from the AI). Follow-up surveys must now be conducted to determine whether the additional 65 colonies predicted to be climate-tolerant remain so to this day, though as was the case with most GRE survey sites, the majority of the reefs were difficult to reach and had never before been surveyed or sampled at the time. Hopefully, funds from

international initiatives like CORDAP can be used by local scientists to periodically check on these corals such that the long-term predictive capacity of the models can be validated.

If these models are only adept at identifying corals that survive only, for instance 1–2 years longer than conspecifics, they may ultimately be of little utility to those looking to stock their nurseries with the most robust corals. However, others have predicted that the thermotolerance of some Palauan corals might actually be increasing over time [31], though these models were not ground-truthed and do not consider key physiological benchmarks of resilience, only organismal abundance. Just as a city with more people is not associated with more resilient citizens, high-coral cover reefs are no more climate-resilient; acroporids in particular have struggled to recover after recent disturbances [32]. As it is unlikely that adaptation is keeping pace with the rapid rate of seawater temperature rise in Palau, the degree to which assisted evolution-based approaches may play a role in boosting coral resilience is currently under investigation there [31] and elsewhere [33]. Perhaps the most resilient *P. acuta* colonies uncovered in our surveys could be cross-bred to yield more thermotolerant larvae for later reef reseeding efforts.

Aside from our omission of samples from Palau's windward reefs, another limitation of this study is that it features only a single species: *P. acuta*. Very different optimal conditions will be associated with other corals, and it is entirely possible that model accuracy for many of them will be too low to be of any value. We know more about *P. acuta* than any other coral [34], and molecules-to-satellites datasets do not exist for any other scleractinian except *Seriatopora hystrix* [35]; the accuracies presented herein likely represent amongst the highest that could be expected for predicting coral resilience to climate change. This is not to say that resilient corals have not been identified in Palau via other approaches. For instance, thermotolerant corals have been found in sheltered regions of the Rock Islands, such as Nikko Bay [36], from where corals were also sampled herein, and the *Porites lobata* genotypes living there are distinct from conspecifics on the outer reefs [37]. Our species-level molecular analysis was too crude to resolve individual *P. acuta* populations, so the DNAs have been sent to colleagues to analyze host coral, dinoflagellate, and microbial genetics at a higher resolution to determine the degree to which adaptation is driving the marked divergence in climate resilience documented [38].

5 Conclusions

By tapping into a dataset featuring molecular and physiological data, as well as simple, easy-to-measure survey parameters, we generated two machine-learning-based models for accurately predicting the climate resilience of the model coral *P. acuta* in Palau. Accuracies were ~90%, and colony size, depth, and local coral cover and diversity were all important predictors of pocilloporid resilience. Host coral genetics surely play a role (i.e., adaptation), as well, especially given the wide diversity of habitats and vast spatial extent of the survey [39]. Although a colony's genotype could likely never be discerned *in situ* by a diver, knowing whether distinct populations tend to be those of highest resilience, regardless of their habitat preferences and physiological characteristics, will nevertheless be useful information for local practitioners, especially those looking to ensure that restored reefs are both "climate-proofed" and diverse [40, 41]. Based on the machine-learning models developed herein, a practitioner or scientist seeking high-temperature-tolerant *P. acuta* colonies in Palau would target ~15-cm diameter individuals at 10 m on reefs of 20–30% coral cover or slightly smaller colonies (10–11-cm diameter) on relatively deeper reefs (18–19 m).

Acknowledgements We would like to thank the talented team at JMP for assistance with predictive modeling and machine-learning. ABM would like to thank the Fulbright and MacArthur Foundations for supporting his stay in Taiwan, where the laboratory analyses were conducted.

Author contributions Conceptualization, A.B.M.; methodology, A.B.M., A.C.D.; software, A.B.M., A.C.D.; validation, A.B.M., A.C.D.; formal analysis, A.B.M., A.C.D.; investigation, A.B.M., A.C.D.; resources, A.B.M., A.C.D.; data curation, A.B.M., A.C.D.; writing—A.B.M.; writing—review and editing, A.B.M.; visualization, A.B.M.; project administration, A.B.M.; funding acquisition, A.B.M., A.C.D. All authors have read and agreed to the published version of the manuscript.

Funding This research was funded by the Khaled bin Sultan Living Oceans Foundation, as well as the Coral Research and Development Accelerator Platform (CORDAP).

Data availability All data and code can be accessed via the online supplemental data file (Appendix B). All images of the coral reef habitats surveyed, as well as the sampled coral colonies, can be found on coralreefdiagnostics.com. The GUI necessary to run the neural networks (for those without coding or machine-learning knowledge) are also posted on this coral physiology database (<https://coralreefdiagnostics.com/>

[palau-bioprospecting](#)). Precipitated RNAs, DNAs, and proteins (all frozen at -80°C), as well as decalcified fragments of a subset of 30 samples embedded in paraffin, are available for sharing; their whereabouts and other key information (e.g., sample size) are described in Mayfield [42].

Declarations

Ethics approval and consent to participate Not applicable.

Consent to participate Not applicable.

Consent for publication Not applicable.

Competing interests The authors declare no competing interests.

Open Access This article is licensed under a Creative Commons Attribution 4.0 International License, which permits use, sharing, adaptation, distribution and reproduction in any medium or format, as long as you give appropriate credit to the original author(s) and the source, provide a link to the Creative Commons licence, and indicate if changes were made. The images or other third party material in this article are included in the article's Creative Commons licence, unless indicated otherwise in a credit line to the material. If material is not included in the article's Creative Commons licence and your intended use is not permitted by statutory regulation or exceeds the permitted use, you will need to obtain permission directly from the copyright holder. To view a copy of this licence, visit <http://creativecommons.org/licenses/by/4.0/>.

References

1. Reimer JD, Peixoto RS, Davies SW, Traylor-Knowles N, Short ML, Cabral-Tena RA, et al. The fourth global coral bleaching event—where do we go from here? *Coral Reefs*. 2024;43:1121–5.
2. Loya Y, Sakai K, Yamazato K, Nakano Y, Sambali H, van Woesik R. Coral bleaching: the winners and the losers. *Ecol Lett*. 2001;4:122–31.
3. Barshis DJ, Ladner JT, Oliver TA, Seneca FO, Traylor-Knowles N, Palumbi SR. Genomic basis for coral resilience to climate change. *Proc Natl Acad Sci USA*. 2013;110:1387–92. <https://doi.org/10.1073/pnas.1210224110>.
4. Mayfield AB, Chan PH, Putnam HM, Chen CS, Fan TY. The effects of a variable temperature regime on the physiology of the reef-building coral *Seriatopora hystrix*: results from a laboratory-based reciprocal transplant. *J Exp Biol*. 2012;215:4183–95.
5. Mayfield AB. Using tourist diver photos to assess the effects of marine heatwaves on Central Red Sea coral reefs. *Environments*. 2025;12:248.
6. Voolstra CR, Buitrago-López C, Perna G, Cárdenas A, Hume BC, Räddecker N, et al. Standardized short-term acute heat stress assays resolve historical differences in coral thermotolerance across microhabitat reef sites. *Glob Change Biol*. 2020;26(8):4328–43.
7. Liu G, Heron SF, Eakin CM, Muller-Karger FE, Vega-Rodriguez M, Guild LS, et al. Reef-scale thermal stress monitoring of coral ecosystems: new 5-km global products from NOAA Coral Reef Watch. *Remote Sens*. 2014;6(11):11579–606.
8. Bachman SD, Kleypas JA, Erdmann M, Setyawan E. A global atlas of potential thermal refugia for coral reefs generated by internal gravity waves. *Front Mar Sci*. 2022;9:921879. <https://doi.org/10.3389/fmars.2022.921879>.
9. Mayfield AB, Dempsey AC. AI-driven coral reef bioprospecting in the Republic of Palau. *Platax*. 2024;21:1–30.
10. Carlton R, Dempsey AC, Lubarsky K, Lindfield S, Faisal M, Purkis S. Global Reef Expedition: the Republic of Palau. Final Report. Khaled bin Sultan Living Oceans Foundation, vol. 12, Annapolis; 2020.
11. Purkis SJ, Gleason ACR, Purkis CR, Dempsey AC, Renaud PG, Faisal M, et al. High-resolution habitat and bathymetry maps for 65,000 sq. km of Earth's remotest coral reefs. *Coral Reefs*. 2019;38:467–88.
12. Mayfield AB, Chen CS, Dempsey AC. Biomarker profiling in reef corals of Tonga's Ha'apai and Vava'u Archipelagos. *PLoS ONE*. 2017;12:e0185857.
13. Mayfield AB, Chen CS, Dempsey AC. Identifying corals displaying aberrant behavior in Fiji's Lau Archipelago. *PLoS ONE*. 2017;12:e0177267.
14. Mayfield AB, Dempsey AC, Chen CS, Lin C. Expediting the search for climate-resilient reef corals in the Coral Triangle with artificial intelligence. *Appl Sci*. 2022;12:12955.
15. Colin PL. Marine Environments of Palau. 1st ed. Honolulu: Mutual Publishing; 2009.
16. Johnston EC, Forsman ZH, Flot J-F, Schmidt-Roach S, Pinzón JH, Knapp ISS, et al. A genomic glance through the fog of plasticity and diversification in *Pocillopora*. *Sci Rep*. 2017;7:5991. <https://doi.org/10.1038/s41598-017-06085-3>.
17. Siebeck UE, Marshall NJ, Klüter A, Hoegh-Guldberg O. Monitoring coral bleaching using a colour reference card. *Coral Reefs*. 2006;25:453–60. <https://doi.org/10.1007/s00338-006-0123-8>.
18. Mayfield AB, Wang LH, Tang PC, Hsiao YY, Fan TY, Tsai CL, et al. Assessing the impacts of experimentally elevated temperature on the biological composition and molecular chaperone gene expression of a reef coral. *PLoS ONE*. 2011;6:e26529.
19. Thomas L, Stat M, Evans RD, Kennington WJ. A fluorescence-based quantitative real-time PCR assay for accurate *Pocillopora damicornis* species identification. *Coral Reefs*. 2016;35:895–9.
20. Correa AMS, McDonald MD, Baker AC. Development of clade-specific *Symbiodinium* primers for quantitative PCR (qPCR) and their application to detecting clade D symbionts in Caribbean corals. *Mar Biol*. 2009;156:2403–11.
21. Putnam HM, Mayfield AB, Fan TY, Chen CS, Gates RD. The physiological and molecular responses of larvae from the reef-building coral *Pocillopora damicornis* exposed to near-future increases in temperature and $p\text{CO}_2$. *Mar Biol*. 2013;160:2157–73.
22. Mayfield AB, Wang YB, Chen CS, Chen SH, Lin CY. Compartment-specific transcriptomics in a reef-building coral exposed to elevated temperatures. *Mol Ecol*. 2014;23:5816–30.

23. Mayfield AB, Chen CS, Dempsey AC. The molecular ecophysiology of closely related pocilloporid corals of New Caledonia. *Platax*. 2017;14:1–45.
24. Mayfield AB. Machine-learning-based proteomic predictive modeling with thermally challenged Caribbean reef corals. *Diversity*. 2022;14:33.
25. McClanahan TR, Donner SD, Maynard JA, MacNeil MA, Graham NAJ. Prioritizing key resilience indicators to support coral reef management in a changing climate. *PLoS ONE*. 2012;2012:e42884. <https://doi.org/10.1371/journal.pone.0042884>.
26. Rubin E, Enochs I, Foord C, Kolodziej G, Basden I, Manzello DP, et al. Molecular mechanisms of coral persistence within highly urbanized locations in the Port of Miami, Florida. *Front Mar Sci*. 2021;8:695236. <https://doi.org/10.3389/fmars.2021.695236>.
27. Anderson KD, Cantin NE, Heron SF, Pisapia C, Pratchett M. Variation in growth rates of branching corals along Australia's Great Barrier Reef. *Sci Rep*. 2017;7:2920. <https://doi.org/10.1038/s41598-017-02920-1>.
28. Mayfield AB, Chen CS. Enabling coral reef triage via molecular biotechnology and artificial intelligence. *Platax*. 2019;16:23–47.
29. Mayfield AB, Chen YJ, Lu CY, Chen CS. The proteomic response of the reef coral *Pocillopora acuta* to experimentally elevated temperature. *PLoS ONE*. 2018;13:e0192001. <https://doi.org/10.1371/journal.pone.0192001>.
30. Chen TY, Hwang GW, Lin HJ, Mayfield AB, Chen CP. The development of a habitat suitability model for sub-tropical tidal flat fiddler crabs. *Ocean Coastal Manag*. 2019;182:104931. <https://doi.org/10.1016/j.ocecoaman.2019.104931>.
31. Lachs L, Donner SD, Mumby PJ, Bythell JC, Humanes A, East HK, et al. Emergent increase in coral thermal tolerance reduces mass bleaching under climate change. *Nat Commun*. 2023;14:4939. <https://doi.org/10.1038/s41467-023-40601-6>.
32. Lachs L, Biondi P, Gouezo M, Nestor V, Olsudong D, Guest J, et al. Demographic recovery of corals at a wave-exposed reef following catastrophic disturbance. *Coral Reefs*. 2024;43:193–9. <https://doi.org/10.1007/s00338-024-02464-1>.
33. van Oppen MJH, Oliver JK, Putnam HM, Gates RD. Building coral reef resilience through assisted evolution. *Proc Natl Acad Sci U S A*. 2015;112:2307–13. <https://doi.org/10.1073/pnas.1422301112>.
34. Mayfield AB, Fan TY, Chen CS. Physiological acclimation to elevated temperature in a reef-building coral from an upwelling environment. *Coral Reefs*. 2013;32:909–21. <https://doi.org/10.1007/s00338-013-0909-2>.
35. Mayfield AB, Chen YJ, Lu CY, Chen CS. Exploring the environmental physiology of the Indo-Pacific reef coral *Seriatopora hystrix* using differential proteomics. *Open J Mar Sci*. 2018;8:223–52. <https://doi.org/10.4236/ojms.2018.82023>.
36. Woesik Rv, Houk P, Isechal AL, Idechong JW, Victor S, Golbuu Y. Climate-change refugia in the sheltered bays of Palau: analogs of future reefs. *Ecol Evol*. 2012;2:2474–84. <https://doi.org/10.1002/ece3.363>.
37. Rivera HE, Cohen AL, Thompson JR, Baums IB, Fox MD, Meyer-Kaiser KS. Palau's warmest reefs harbor thermally tolerant corals that thrive across different habitats. *Commun Biol*. 2022;5:1394. <https://doi.org/10.1038/s42003-022-04315-7>.
38. Palumbi SR, Walker NS, Hanson E, Armstrong K, Lippert M, Cornwell B, et al. Small-scale genetic structure of coral populations in Palau based on whole mitochondrial genomes: implications for future coral resilience. *Evol Appl*. 2023;16(2):518–29. <https://doi.org/10.1111/eva.13509>.
39. Baums IB. A restoration genetics guide for coral reef conservation. *Mol Ecol*. 2008;17(12):2796–811. <https://doi.org/10.1111/j.1365-3113.2008.03611.x>.
40. Quigley KM, Hein M, Suggett DJ. Translating the 10 golden rules of reforestation for coral reef restoration. *Conserv Biol*. 2022;36(4):e13890. <https://doi.org/10.1111/cobi.13890>.
41. Quigley KM, Bay LK, van Oppen MJH. Genome-wide SNP analysis reveals an increase in adaptive genetic variation through selective breeding of coral. *Mol Ecol*. 2020;29(12):2176–88. <https://doi.org/10.1111/mec.15555>.
42. Mayfield AB. Establishment of a long-term reef-building coral biopsy archive as a tool for the marine biology research community. *Platax*. 2023;20:7–30.

Publisher's Note Springer Nature remains neutral with regard to jurisdictional claims in published maps and institutional affiliations.